

Camouflaged Instance Segmentation: Dataset and Benchmark Suite

Trung-Nghia Le¹, Yubo Cao², Tan-Cong Nguyen^{3,4}, Khanh-Duy Nguyen^{3,5}, Thanh-Toan Do⁶, Minh-Triet Tran^{3,7,8}, and Tam V. Nguyen^{*2}

¹National Institute of Informatics, Japan

²University of Dayton, US

³Vietnam National University, Ho Chi Minh City, Vietnam

⁴University of Social Sciences and Humanities, Ho Chi Minh City, Vietnam

⁵University of Information Technology, VNU-HCM, Vietnam

⁶University of Liverpool, UK

⁷University of Science, Ho Chi Minh City, Vietnam

⁸John von Neumann Institute, VNU-HCM, Vietnam

Abstract—This paper pushes the envelope on camouflaged regions to decompose them into meaningful components, namely, camouflaged instances. To promote the new task of camouflaged instance segmentation, we introduce a new large-scale dataset, namely CAMO++, by extending our preliminary CAMO dataset (camouflaged object segmentation) in terms of quantity and diversity. The new dataset substantially increases the number of images with hierarchical pixel-wise ground-truths. We also provide a benchmark suite for the task of camouflaged instance segmentation. In particular, we conduct extensive evaluation of state-of-the-art instance segmentation detectors on our newly constructed CAMO++ dataset in various scenarios. The dataset, evaluation suite, and benchmark will be publicly available at our project page.¹

Index Terms—Camouflaged instance, instance segmentation, benchmark suite

I. INTRODUCTION

The term “camouflage” was originally used to describe the behavior of an animal trying to hide itself from its surroundings to hunt or avoid being hunted [1], namely naturally camouflaged objects [2]. Human adopted this and began to apply it widely on the battlefield. For example, soldiers and war equipment are applied the camouflage effect by dressing or coloring their appearance to blend them with their surroundings, namely artificially camouflaged objects [2]. Autonomously identifying camouflaged objects is beneficial in various fields of computer vision (search-and-rescue work; wild species discovery and preservation [2]), medical diagnostic (polyps detection and segmentation [3]; COVID-19 infection identification from lung x-ray [4]), media forensic (manipulated image/video detection and segmentation [5], [6]).

Early works of camouflage detection [7]–[14], which are based on handcrafted low-level features can work for only a few cases of simple and non-uniform background. Recently, deep learning based detectors [2], [15] have been proposed to tackle the problem of camouflaged object segmentation.

However, these work can perform only at region-level, by mapping each pixel into camouflage/non-camouflage labels, which cannot show the number of camouflaged objects in the scene. None of them targets instance-level segmentation.

In this paper, we promote the new task of **camouflaged instance segmentation**. Camouflaged object is defined as all camouflaged pixels in an image without any further detail information such as the number of objects or semantic meaning [2]. In contrast, *camouflaged instance consists of only meaningful pixels, which cover an object*. To achieve this goal, the new task aims at *simultaneous decomposition of a camouflaged region into meaningful components, namely, camouflaged instances*. Camouflaged instance segmentation is more challenging than conventional camouflaged object segmentation in the sense that it *not only maps each pixels into labels but also sets instance identity for pixels*. To our best knowledge, this is the first work to address camouflaged instance segmentation.

To this end, we introduce the first large-scale dataset specifically designed for the task of camouflaged instance segmentation. The proposed dataset contains 5500 images of human and more than 80 animal species with hierarchically pixel-wise annotation for all images. Our new dataset can be served as a benchmark for not only the camouflaged instance segmentation task, but also the conventional task of camouflaged object segmentation. We also provide a benchmark suite to facilitate the evaluation and advance the task of camouflaged instance segmentation. Particularly, we evaluate and analyze state-of-the-art instance segmentation methods in various scenarios.

We summarize the contribution of this paper as follows:

- We address the new task of **camouflaged instance segmentation** and analyze in-depth challenges of the problem. To our best knowledge, it is the first time that camouflaged instance segmentation is formally defined and explored. Finding camouflaged instances in scenes is a useful task and it can be an interesting problem for the community. A few existing work can perform only

*Corresponding author. *e-mail: tamnguyen@udayton.com*

¹https://sites.google.com/view/ltnghia/research/camo_plus_plus

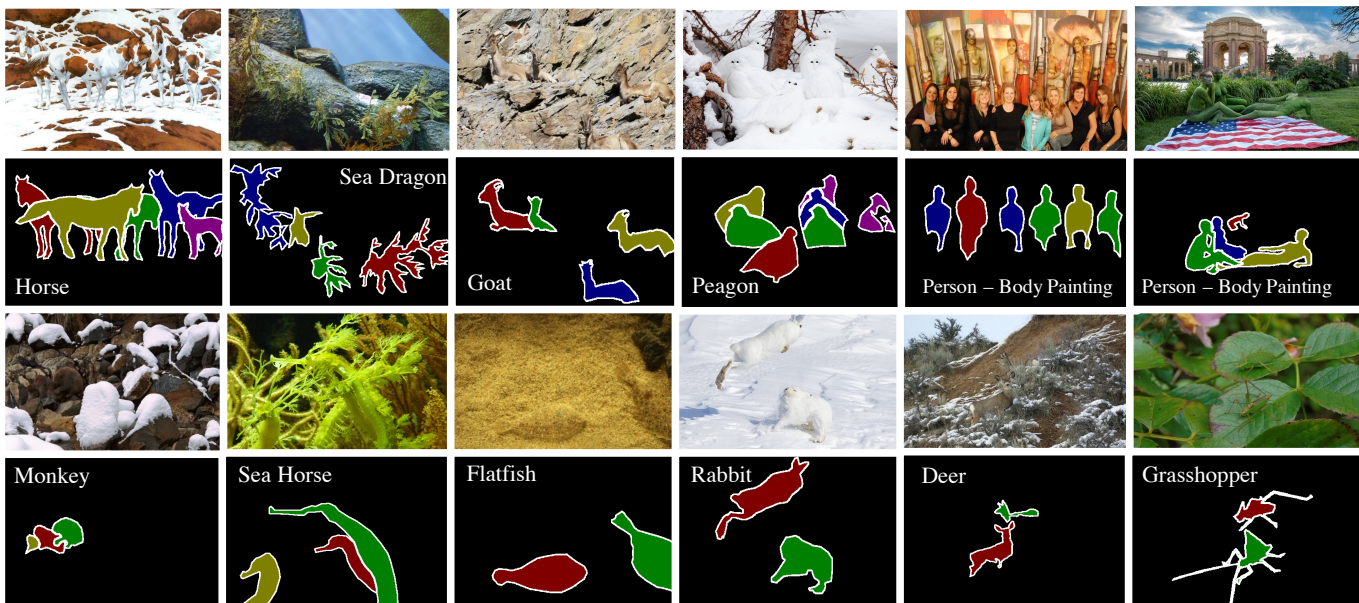


Fig. 1: A few examples from our **Camouflaged Object (CAMO++)** dataset with corresponding pixel-level annotations. ++ means the increment in terms of dataset size and the task compared to our preliminary CAMO dataset [2]. The first row is original images, followed by pixel-wise ground-truth. Each camouflaged instance is illustrated by a distinguished color for the visualization purpose only. Camouflaged instances attempt to conceal their texture into the background. Best viewed in color and with zoom.

camouflaged object segmentation, but no work can at instance-level.

- We present a new image dataset to promote the task of camouflaged instance segmentation. Our newly constructed **Camouflaged Object Plus Plus (CAMO++)** dataset, extended from our preliminary CAMO dataset [2], consists of 5500 images of human and more than 80 animal species, including 2700 camouflage images and 2800 non-camouflage images. All images are hierarchically annotated with bounding-box, meta-category labels, fined-category labels, instance-level labels. Pixel-wise ground-truths are manually annotated for all instances in each image.
- We provide a benchmark suite for the task of camouflaged instance segmentation. In particular, we conduct extensive evaluation of state-of-the-art instance segmentation methods in various scenarios. We further provide in-depth analysis over the experiments. The CAMO++ dataset, evaluation suite, and benchmark will be made available on our website along with the publication².

The remainder of this paper is organized as follows. Section II summarizes the related work. Next, Section III introduces the constructed CAMO++ dataset. Section IV then reports benchmark suite and evaluation of baselines on the newly constructed dataset. Finally, Section V draws the conclusion and paves the way for future work.

II. RELATED WORK

A. Camouflaged Object Segmentation

A camouflaged object is defined as all camouflaged pixels in an image without any further detail information such as the number of objects or semantic meaning [2]. Although camouflaged object recognition also has a wide range of applications, in the literature, this research field has not been well explored in the literature. Early works related to camouflage had been dedicated to detecting the foreground region even when some of their texture is similar to the background [7]–[9]. These works distinguish foreground and background based on simple features such as color, intensity, shape, orientation, and edge. A few methods based on handcrafted low-level features are proposed to tackle the problem of camouflage detection [10]–[14]. However, all these methods work for only a few cases of simple and non-uniform background, thus their performances are unsatisfactory in camouflaged object segmentation due to strong similarity between the foreground and the background.

Recently, Le *et al.* [2] proposed an end-to-end network, dubbed ANet, for camouflaged object segmentation through integrating classification information into segmentation. The potential idea of utilizing classification into segmentation can be useful when applying for multiple regional segmentation in appropriate ways. Follow the same direction, Fan *et al.* [15] later developed SINet which includes two main modules, namely the search module and the identification module. This work is based on simulated hunting, where a predator will first judge whether a potential prey exists, *i.e.*, it will search for a prey; then, the target animal can be identified; and, finally, it can be caught. On the other hand, Yan *et al.* [16]

²https://sites.google.com/view/ltnghia/research/camo_plus_plus

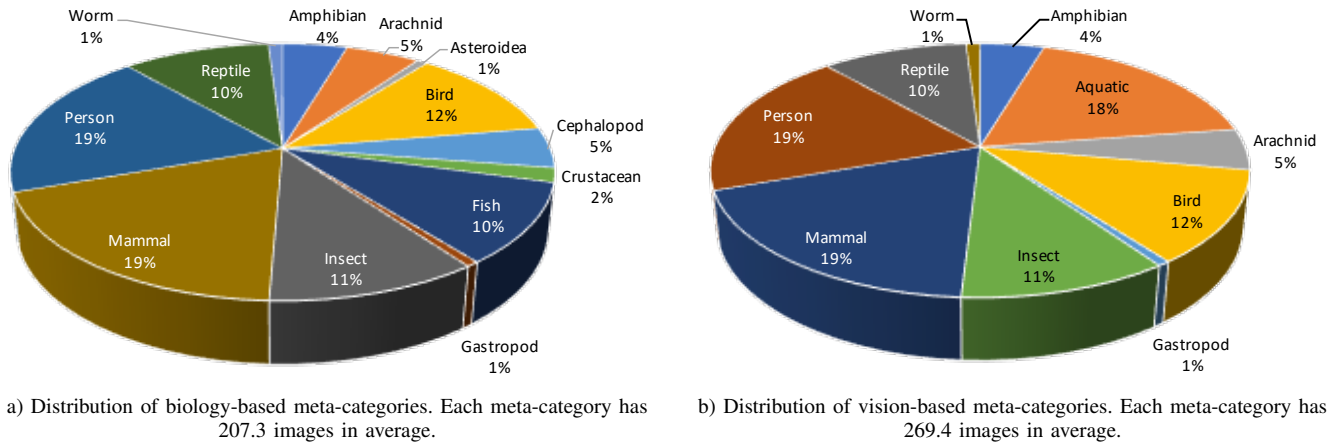


Fig. 3: Distribution of meta-categories in CAMO++ dataset.

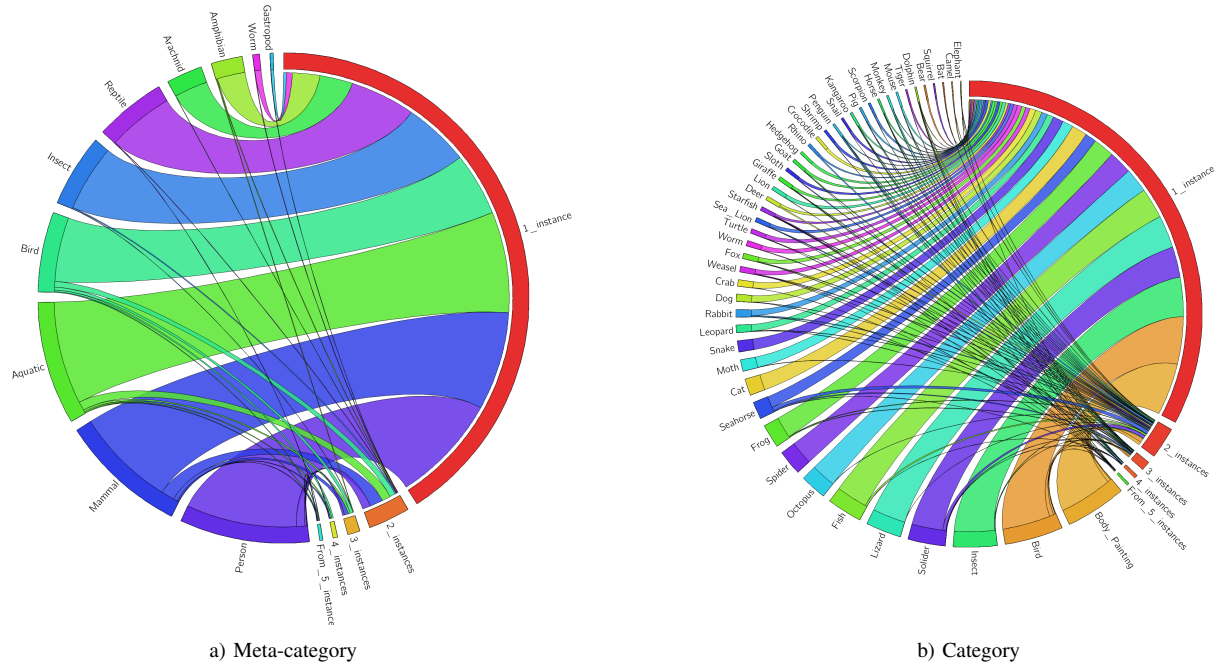


Fig. 4: Mutual dependencies among categories in CAMO++ dataset. Best viewed in color and with zoom.

and CenterMask [36] are extended from YOLACT. These methods aims to blend cropped prototype masks with a finer-grained mask within each bounding-box. CenterMask [36] adds a spatial attention-guided mask branch to anchor-free one stage object detector (FCOS [33]). BlendMask [35] first predicts dense per-pixel position-sensitive instance features with very few channels, and then merges attention maps for each instance through a blender module. In addition, PolarMask [37] formulates the instance segmentation problem as predicting contour of instance through instance center classification and dense distance regression in a polar coordinate. Meanwhile, EmbedMask [38] generates embeddings for pixels and proposals to assign pixels to the mask of the proposal if their embedding are similar. TensorMask [39] investigates the paradigm of dense sliding window instance segmentation, using structured 4D tensors to represent masks over a spatial

domain.

According to our best of knowledge, no existing work has been proposed for camouflaged instance segmentation officially. Obviously we notice the lack of a large-scale dataset for the training and testing purposes. Therefore, in this paper, we build a benchmark for the task of camouflaged instance segmentation by training instance segmentation methods on our newly constructed CAMO++ dataset. We further conduct extensive evaluation of state-of-the-art instance segmentation methods in various scenarios.

III. LARGE-SCALE CAMOUFLAGED INSTANCE DATASET

The core contribution of this paper is our CAMO++ dataset extending our preliminary CAMO dataset [2]. This new large-scale dataset enables us to train and evaluate state-of-the-art methods for the task of camouflaged instance segmentation.

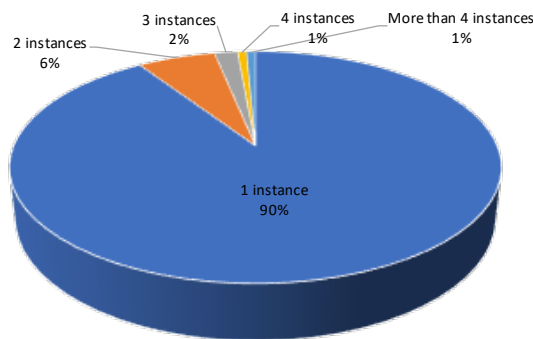


Fig. 5: The density of instances in CAMO++ dataset. Each image has from 1 to 21 instances, and most of them have a single instance.

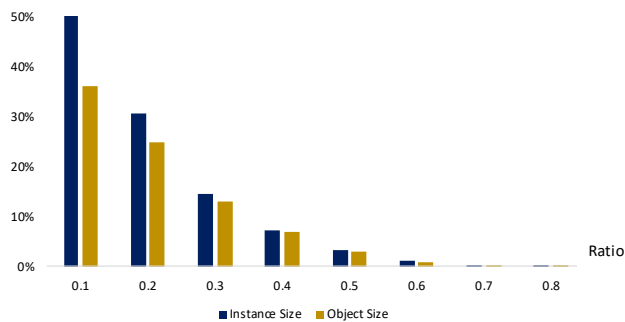


Fig. 6: Distribution of the instance/object size. Object size is computed as total instances in an image. Size of camouflaged instances in CAMO++ dataset is diversity (*i.e.*, tiny, small, medium, large).

A. Dataset Construction

1) *Data Collection*: In order to build the dataset, we initially collected 4000 images in which at least one camouflaged object exists. We collected the images of camouflaged objects from the Internet with different keywords by combining adjective “camouflaged”, “concealed”, “hidden”, with various animals (*e.g.*, cat, dog, seahorse, *etc.*), persons (*e.g.*, soldier, body-painting, *etc.*), and environments (*e.g.*, marine, underwater, mountain, desert, forest, *etc.*).

Then, we manually discarded images with low resolution. We later mixed them with 1250 camouflage images from our preliminary CAMO dataset [2] and manually discarded duplication. Finally, we ended up with 2700 images.

2) *Data Annotation*: We asked ten annotators to differentiate camouflaged instances and annotate these instances in all images individually using a custom-designed interactive segmentation tool. On average, each person takes 5-20 minutes to annotate one image depending on its complexity. The annotation stage spanned about two months. The outcome of this process is the binary mask and its hierarchical categories for each instance (cf. Fig. 1).

B. Dataset Specifications and Statistics

We describe in this section the **Camouflaged Object Plus (CAMO++)** dataset designed explicitly for the task of

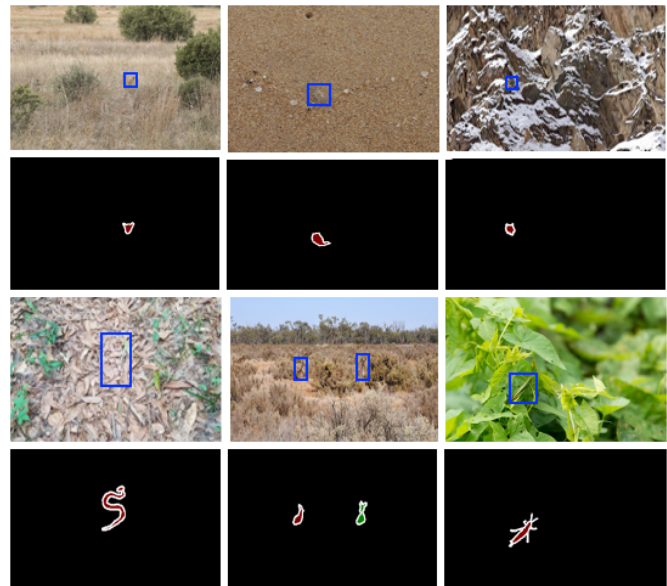


Fig. 7: Examples of tiny camouflaged instances. Each instance is overlaid by a distinguished color for the visualization purpose only. Best viewed in color and with zoom.

camouflaged instance segmentation. ++ means the increment in terms of dataset size and the task compared to CAMO dataset [2]. Some examples are shown in Fig. 1 with the corresponding ground-truth label annotations.

Category Diversity. In CAMO++, we focus on camouflaged human and camouflaged animals with various pieces. Figure 2a highlights diversity in biology-inspired categorization. The CAMO++ dataset consists of hierarchically biological 13 meta-categories (*e.g.*, amphibian, arachnid, asteroidea, bird, cephalopod, crustacean, fish, gastropod, insect, mammal, person, reptile, and worm) and 83 categories (cf. Fig. 2a). Each category contains 32.5 images in average. Figure 3a shows ratio of biological meta-categories in the CAMO++ dataset, where each meta-category contains 207.3 images in average.

However, biological categorization has the disadvantage that the number of samples of categories may not be sufficient to train and evaluate methods, especially deep learning methods. To guarantee the number of samples for training and evaluating methods, we re-organize categories based on vision features (*i.e.*, appearance) in combination with biological features (*i.e.*, behavior, living environment). We built a new list of 10 meta-categories (*e.g.*, amphibian, aquatic, arachnid, bird, gastropod, insect, mammal, person, reptile, and worm) and 47 categories. Figure 2b show 2 camouflaged human categories (*e.g.*, body painting and soldier) and 45 camouflaged animal categories (*e.g.*, frog, crab, dolphin, fish, octopus, seahorse, shrimp, starfish, scorpion, spider, bird, penguin, snail, insect, moth, bat, bear, camel, cat, deer, dog, elephant, fox, giraffe, goat, hedgehog, horse, kangaroo, leopard, lion, monkey, mouse, pig, rabbit, rhino, sea lion, sloth, squirrel, tiger, weasel, crocodile, lizard, snake, turtle, and worm), where each category consist of 57.3 images in average. The ratios for each meta-category are shown in Fig. 3b, in which each meta-category contains 269.4 images in average.

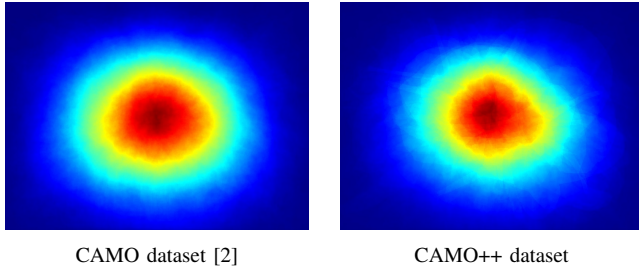


Fig. 8: Center bias comparison between CAMO and CAMO++ datasets.

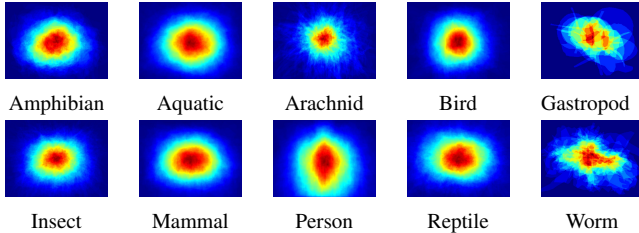


Fig. 9: Center bias of meta-categories in CAMO++ dataset.

TABLE I: Distribution of images in CAMO++ dataset.

	Training Set	Testing Set	Total
Camouflage Image	1700	1000	2700
Non-camouflage Image	1800	1000	2800
Total	3500	2000	5500

Diversity of CAMO++ dataset enables a comprehensive understanding of camouflage instances in both biology and computer vision.

Instance Density. Figure 4 shows mutual dependencies of the number of instances at each meta-category and each category. In our CAMO++ dataset, each image has from 1 to 21 instances. Figure 5 illustrates ratios of number of instances in an image over the CAMO++ dataset. It is noteworthy that a number of images with multiple instances, including separate single instances and spatially connected/overlapping instances, take 10% of the dataset. 6% of the images have two instances. Meanwhile, 2% and 1% of the images contain three and four instances, respectively. The remainder, 1% of images, is with more than four instances (Fig. 5). This makes our CAMO++ dataset more challenging for the camouflaged instance segmentation task.

Instance Size. The size of an instance/object is defined as the proportion of its pixels to the entire image. We remark that an object, which is corresponding to conventional camouflaged object segmentation task, is treated as total areas of all camouflaged instances in an image. Figure 6 shows distribution of the instance/object size over the CAMO++ dataset. The CAMO++ dataset contains a large number of small and medium instances. Medium instances with size from 0.1 to 0.3 take 90% of number of instances, meanwhile the small instance with the size smaller than 0.1 takes 51% of the number of instances. It is also noteworthy that CAMO++ dataset consists of the number of tiny instances (cf. Fig. 7),



Fig. 10: A few examples of non-camouflage images. Each instance is overlaid by a distinguished color for the visualization purpose only. Best viewed in color and with zoom.

which makes our dataset more challenging for camouflaged instance segmentation.

Center Bias. Figure 8 depicts the distributions of object centers in normalized image coordinates over all images in CAMO dataset [2] and our proposed CAMO++ dataset. Camouflage images are biased to the center of images. This can be explained that camouflage images are usually cropped for camouflaged instances nearly at the center for people to identify those concealed instances. In addition, the center bias of meta-categories in the CAMO++ dataset are presented in Fig. 9.

Our newly constructed CAMO++ dataset also inherits challenging attributes from the CAMO dataset [2], such as *object appearance*, *background clutter*, *shape complexity*, *object occlusion*, and *distraction*. Readers please refer to the CAMO dataset [2] for more details.

C. Dataset Splits

We randomly split 2700 camouflage images into separate training and testing sets, in which the training set consists of 1700 images, and the testing set consists of 1000 images.

We also manually select 2800 images from the training set and validation set of the LVIS dataset [40], which contains at least a human or animal instance. We manually selected the images to guarantee they do not contain any camouflaged instance, namely non-camouflage images, to support false positive segmentation. These images with the corresponding ground-truth are randomly split into training and testing sets with 1800 images and 1000 images, respectively. Figure 10 shows examples of the non-camouflage images. Table I shows

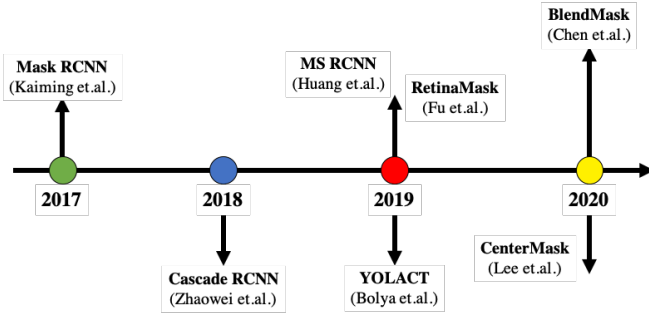


Fig. 11: Timeline of benchmarked instance segmentation methods.

distribution of images in our newly constructed CAMO++ dataset.

IV. BENCHMARK SUITE

In addition to our large-scale CAMO++ database, we conduct a competitive benchmark for camouflaged instance segmentation. To this end, we trained and tested various instance segmentation methods (*i.e.*, Mask RCNN [23], Cascade RCNN [28], MS RCNN [27], RetinaMask [30], YOLACT [34], CenterMask [36], BlendMask [35], SOLO [41], SOLO2 [42], and CondInst [43]) on subsets as in Section III-C. Figure 11 shows the timeline of the benchmarked state-of-the-art methods. To demonstrate the generalization of methods, we employ different backbones, namely, ResNet50-FPN [44], ResNet101-FPN [44], and ResNeXt101-FPN [45], for each instance segmentation methods.

We trained models on PCs with 32GB RAM memory and Tesla P100 GPUs. Methods were fine-tuned from the MSCOCO pre-trained models using default public configurations provided by authors.

A. Evaluation Measures

All reported results follow standard COCO-style Average Precision (AP) metrics that include AP (averaged over IoU thresholds from 50% to 95%), AP_{50} (AP for IoU threshold 50%), AP_{75} (AP for IoU threshold 75%) [46], and AP_{Small} , AP_{Medium} , AP_{Large} (AP at different scales). We also reported results on Average Recall (AR) metrics that include AR_1 , AR_{10} , AR_{100} (AR given number of detection per image) [46], and AR_{Small} , AR_{Medium} , AR_{Large} (AR at different scales).

B. Benchmarking Results

We evaluate instance segmentation methods on different settings, namely:

- Setting 1: training and testing on only camouflage images (denoted by CAMO-only Images). In this experimental setting, we assume that camouflaged objects appear in every images.
- Setting 2: training and testing on both camouflage and non-camouflage images (denoted by CAMO++ Images).

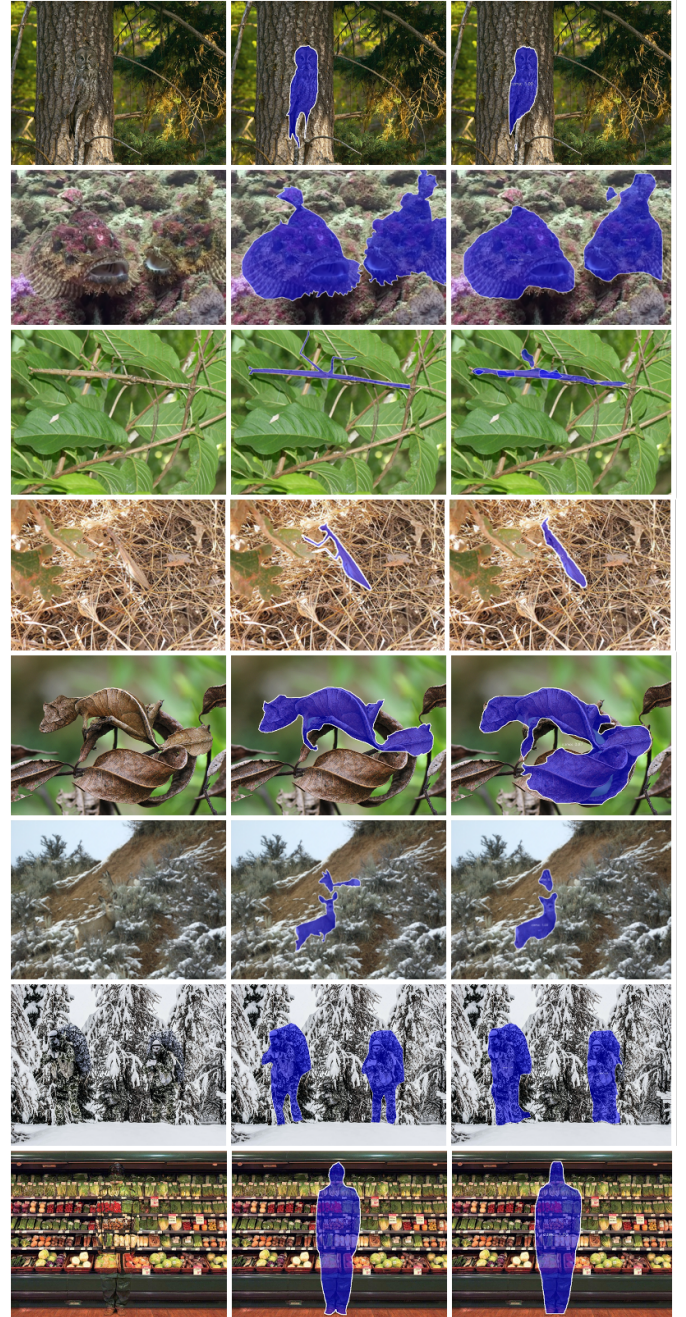


Fig. 12: Visualized results of Cascade RCNN [28], the best method trained on camouflage images. From left to right: the original image is followed by overlaid ground truth and the result of Cascade RCNN. Best viewed in color and with zoom. More results are on our website.

This experimental setting simulates the real-world, where camouflaged instances do not always exist in images.

- Setting 3: training on a combination of camouflage and non-camouflage images and testing on only camouflage image. This experimental setting aims to exploiting ability of utilizing non-camouflage images to segment camouflaged instances.

The detailed performance is discussed in the subsections below.

TABLE II: The results of training and testing on CAMO-only images. The two best results are shown in **blue** and **red**, respectively.

Method	Backbone	Average Precision (AP)			AP Across Scales			Average Recall (AR)			AR Across Scales		
		AP	AP ₅₀	AP ₇₅	AP _S	AP _M	AP _L	AR ₁	AR ₁₀	AR ₁₀₀	AR _S	AR _M	AR _L
Mask RCNN [23]	ResNet50-FPN	24.4	52.5	21.1	6.5	18.7	26.3	26.7	33.1	33.1	6.7	25.1	35.7
Mask RCNN [23]	ResNet101-FPN	23.7	51.5	19.6	7.0	16.2	26.0	26.3	32.0	32.1	7.8	23.8	34.7
Mask RCNN [23]	ResNeXt101-FPN	31.2	62.7	29.4	8.6	22.3	34.1	32.8	38.6	38.7	11.7	28.1	42.0
Cascade RCNN [28]	ResNet50-FPN	25.1	51.8	21.9	4.8	17.4	27.7	27.0	34.4	34.5	4.4	24.7	37.7
Cascade RCNN [28]	ResNet101-FPN	26.7	53.8	23.6	11.4	18.9	29.2	28.8	36.5	36.5	12.2	25.8	39.8
Cascade RCNN [28]	ResNeXt101-FPN	33.6	66.0	30.7	11.7	25.0	36.5	34.0	44.6	45.0	13.9	35.0	48.2
MS RCNN [27]	ResNet50-FPN	27.0	54.3	24.5	11.7	19.6	29.3	27.5	33.4	3.5	1.33	26.1	35.8
MS RCNN [27]	ResNet101-FPN	28.1	55.6	26.2	9.3	21.7	30.2	29.0	35.0	35.4	10.0	27.7	37.8
MS RCNN [27]	ResNeXt101-FPN	31.0	60.4	29.2	8.0	24.2	33.2	32.4	38.4	38.6	10.0	29.8	41.5
RetinaMask [30]	ResNet50-FPN	21.5	48.2	17.0	14.4	18.5	2.8	25.9	31.5	31.9	16.1	25.6	33.9
RetinaMask [30]	ResNet101-FPN	23.5	50.2	19.5	13.9	20.3	24.9	27.4	33.7	33.9	20.0	28.6	35.6
RetinaMask [30]	ResNeXt101-FPN	25.8	53.1	23.3	13.3	20.5	27.8	29.9	36.6	36.8	13.9	28.7	39.3
YOLACT [34]	ResNet50-FPN	20.6	41.9	17.5	6.5	16.3	22.3	25.8	29.3	29.6	9.4	21.8	32.0
YOLACT [34]	ResNet101-FPN	21.7	42.1	20.0	6.2	17.2	23.5	25.9	30.1	30.1	7.2	22.8	32.4
CenterMask [36]	ResNet50-FPN	19.7	47.1	13.7	6.7	13.8	21.4	22.9	30.7	30.9	11.	26.8	32.3
CenterMask [36]	ResNet101-FPN	23.1	53.3	17.1	9.3	16.3	25.2	26.8	34.9	35.2	26.1	29.0	37.0
CenterMask [36]	ResNeXt101-FPN	26.6	57.4	23.2	7.7	17.0	29.6	29.8	37.1	37.3	10.0	28.7	40.0
BlendMask [35]	ResNet50-FPN	21.7	47.4	18.3	10.3	17.0	23.4	26.1	31.4	31.5	14.4	24.4	33.6
BlendMask [35]	ResNet101-FPN	25.5	53.5	20.6	18.8	20.2	27.3	30.2	35.5	35.6	22.2	26.9	38.1
SOLO [41]	ResNet50-FPN	22.6	46.9	19.3	6.0	8.9	26.5	26.2	28.9	29.0	6.1	13.2	33.6
SOLO [41]	ResNet101-FPN	23.8	48.5	21.3	6.9	12.0	27.3	28.4	30.9	31.0	7.8	15.9	35.4
SOLO [41]	ResNeXt101-FPN	24.3	48.5	22.1	5.8	9.0	28.7	28.9	31.2	31.3	8.3	13.1	36.5
SOLO2 [42]	ResNet50-FPN	22.6	48.1	19.8	4.8	8.9	26.5	26.0	28.3	28.4	5.0	13.2	32.8
SOLO2 [42]	ResNet101-FPN	29.1	53.5	28.3	7.4	13.7	33.5	33.0	35.2	35.3	10.6	18.4	40.2
SOLO2 [42]	ResNeXt101-FPN	30.9	56.2	30.3	5.8	14.3	35.6	34.7	37.3	37.5	8.9	19.1	42.9
CondInst [43]	ResNet50-FPN	29.2	58.7	26.4	12.2	20.7	31.7	32.4	39.2	39.3	13.9	28.2	42.7
CondInst [43]	ResNet101-FPN	31.8	63.4	29.3	19.1	23.1	34.5	34.5	41.7	41.9	21.7	31.6	45.0

1) *Setting 1: Training and Testing on CAMO-only Images:* Table II reports the performance of different methods on the first experimental setting. As can be seen from the table, the better backbones tend to produce better results within the same methods. ResNeXt101-based implementations provide the best performance. In terms of Average Precision (AP), AP₅₀ metrics obviously obtain the highest scores. On the contrary, AP₇₅ metrics yield the lowest scores. Meanwhile, AP_L, AR₁₀₀, AR_L produce the highest scores in terms of AP Across Scales, Average Recall, and AR Across Scales, respectively. In general, the benchmarking methods consistently perform across the performance metrics. In other words, the methods performing well in one performance metrics tend to perform well for the rest.

We later take a closer look to the performance of the state-of-the-art instance segmentation methods. The most popular method, Mask RCNN [23] well performs in the task. MS RCNN [27] slightly surpasses Mask RCNN in the two backbones, *i.e.*, ResNet50 and ResNet101. In the meantime, Cascade RCNN [28] achieves the best performance across all metrics. The cascade paradigm proposed in [28] well performs on camouflaged instances. The recently proposed single-stage methods, *i.e.*, YOLACT [34] and its variants, show the inferior results compared to the previously mentioned methods. The main reason is that these methods rely on the single-stage object detector. In fact, they focus on real-time performance rather than precision or recall measurement. Above all, Cas-

cade RCNN and Mask RCNN with ResNeXt101 backbone achieve the top two performance over other methods. Figure 12 illustrates results of Cascade RCNN with ResNeXt101 backbone.

2) *Setting 2: Training and Testing on CAMO++ Images:* Table III details the performance of different methods on the second experimental setting. The most popular method, Mask RCNN [23] competitively performs in the task. However, RetinaMask [30] slightly outperforms Mask RCNN with a small margin. In the meantime, Cascade RCNN [28] achieves the good performance across all metrics. MS RCNN [27] obtains the best performance in this setting. MS RCNN contains a network block which learns the quality of the predicted instance masks. This may help boost the performance of MS RCNN while training and testing on CAMO++ images. Other methods, *i.e.*, YOLACT, CenterMask, and BlendMask, still show the inferior results compared to the previously mentioned methods. The single stage object detector is the reason of this performance. In fact, they mainly focus on the real-time performance rather than the precision or recall measurement. Above all, Cascade RCNN and MS RCNN with ResNeXt101 backbone obtain the top two performance over other methods. MS RCNN reaches the best performance in terms of APs whereas Cascade RCNN achieves the top scores in terms of ARs. Figure 13 shows the visual comparison of different methods with the same ResNet50 backbone. We remark that we visualize only ResNet50 backbone since this backbone is

TABLE III: The results of training and testing on CAMO++ images. The two best results are shown in **blue** and **red**, respectively.

Method	Backbone	Average Precision (AP)			AP Across Scales			Average Recall (AR)			AR Across Scales		
		AP	AP ₅₀	AP ₇₅	AP _S	AP _M	AP _L	AR ₁	AR ₁₀	AR ₁₀₀	AR _S	AR _M	AR _L
Mask RCNN [23]	ResNet50-FPN	16.1	36.4	12.9	4.0	19.0	34.1	14.7	22.3	24.3	6.4	28.6	46.0
Mask RCNN [23]	ResNet101-FPN	17.1	37.6	14.5	4.7	20.5	35.3	15.5	23.1	25.3	6.8	31.0	47.1
Mask RCNN [23]	ResNeXt101-FPN	19.9	42.2	16.7	6.8	22.5	39.7	18.5	25.2	27.0	8.4	31.4	50.2
Cascade RCNN [28]	ResNet50-FPN	16.9	36.6	13.9	3.6	20.0	35.8	15.5	23.5	25.6	5.3	30.5	48.3
Cascade RCNN [28]	ResNet101-FPN	17.6	37.9	15.0	4.7	21.6	37.0	15.9	24.3	26.7	8.8	31.6	50.0
Cascade RCNN [28]	ResNeXt101-FPN	21.5	44.0	19.7	6.3	26.1	40.3	18.6	28.8	32.0	11.9	39.2	55.2
MS RCNN [27]	ResNet50-FPN	19.1	38.1	18.0	8.3	23.2	35.4	15.5	23.0	25.9	12.1	31.3	44.9
MS RCNN [27]	ResNet101-FPN	20.0	38.4	18.9	8.6	24.6	37.2	16.2	24.1	26.9	12.5	33.3	47.2
MS RCNN [27]	ResNeXt101-FPN	22.9	44.2	21.8	11.8	27.8	39.9	18.0	26.9	30.5	14.6	37.1	50.2
RetinaMask [30]	ResNet50-FPN	17.4	37.5	14.5	8.8	21.8	32.9	15.1	23.8	27.7	12.5	33.6	46.3
RetinaMask [30]	ResNet101-FPN	18.0	38.2	15.7	10.3	22.2	33.9	16.1	24.9	28.5	18.1	35.6	47.8
RetinaMask [30]	ResNeXt101-FPN	20.0	41.2	17.6	12.4	24.9	36.9	17.8	26.6	30.4	16.6	38.0	50.5
YOLACT [34]	ResNet50-FPN	14.7	31.4	12.9	5.1	19.8	32.8	14.7	20.9	22.8	11.5	29.2	43.9
YOLACT [34]	ResNet101-FPN	15.9	32.4	14.2	8.6	19.6	36.1	16.1	22.2	23.6	13.0	28.1	47.1
CenterMask [36]	ResNet50-FPN	14.9	34.9	11.1	9.5	18.6	27.5	13.3	22.9	26.6	14.5	34.8	43.2
CenterMask [36]	ResNet101-FPN	15.9	35.7	12.8	8.8	19.4	29.9	14.8	23.5	26.1	14.5	33.6	44.5
CenterMask [36]	ResNeXt101-FPN	19.9	42.4	17.5	9.0	24.4	33.9	16.9	26.8	30.3	15.2	38.5	47.7
BlendMask [35]	ResNet50-FPN	18.2	38.6	15.4	9.8	23.7	34.1	15.9	24.7	28.6	15.3	35.7	47.7
BlendMask [35]	ResNet101-FPN	20.3	40.6	18.2	12.1	26.5	38.1	17.3	25.6	28.9	14.9	36.7	50.9
SOLO [41]	ResNet50-FPN	14.8	29.7	13.6	6.3	20.6	31.6	13.9	21.4	23.8	8.8	31.0	45.9
SOLO [41]	ResNet101-FPN	18.3	36.2	16.5	5.9	22.5	35.0	17.3	25.5	27.4	12.2	33.5	49.5
SOLO [41]	ResNeXt101-FPN	19.3	37.3	18.2	9.3	21.1	37.5	18.7	26.8	28.6	12.0	33.2	52.7
SOLO2 [42]	ResNet50-FPN	17.8	34.2	16.4	7.0	22.3	36.5	15.9	24.0	26.0	10.4	31.7	49.3
SOLO2 [42]	ResNet101-FPN	24.0	43.7	23.6	13.3	28.6	45.2	20.7	30.6	33.5	16.6	40.6	59.6
SOLO2 [42]	ResNeXt101-FPN	24.8	43.3	24.5	12.0	27.6	47.0	22.1	31.1	34.2	16.5	40.3	61.2
CondInst [43]	ResNet50-FPN	20.9	42.7	18.6	12.3	24.6	39.2	18.3	26.6	30.1	16.5	37.8	51.5
CondInst [43]	ResNet101-FPN	22.5	43.7	20.2	12.8	27.3	42.8	19.9	28.5	31.6	15.3	38.6	55.8

most popular in segmentation methods.

3) *Setting 3: Training on CAMO++ and Testing on CAMO-only Images*: Table IV reports the performance of different methods on the third experimental setting. Similar as discussed in Section IV-B1, Mask RCNN [23] well performs in this setting. Meanwhile, MS RCNN [27] obtains better performance than that of Mask RCNN. Cascade RCNN [28] again achieves the best performance across all metrics. Note that this setting only runs testing on CAMO-only images.

The other state-of-the-art methods, namely, RetinaMask, YOLACT, CenterMask, and BlendMask, show the inferior results compared to the previously mentioned methods. We observe that by adding the non-camouflaged instances, the finetuned models achieve better performance in detecting and segmenting the camouflaged instances. This shows that the training non-camouflaged instances really help boost the performance. Once again, Cascade RCNN and MS RCNN are the top two performers in this experiment. In particular, Cascade RCNN with ResNeXt101 backbone achieves the best performance over other methods. The more advanced backbones in the future will definitely help increase the performance.

We observe that when training on CAMO++ images with two backbones, namely, ResNet50 and ResNet101, BlendMask [35] is better than all two-stage methods on both two test settings (as seen in Table III and Table IV). As discussed above, images of non-camouflage instances are really helpful in training camouflaged instance segmentation methods. Here, it is interesting that BlendMask can be boosted thanks to

the combined data more significantly than other benchmarked methods.

C. Failure Cases and Discussion

In this subsection, we discuss about the failure cases of state-of-the-art instance segmentation methods in camouflaged instance segmentation. Figure 14 shows the exemplary failure cases in CAMO++ dataset. The top five rows are related to wrong segmentation of camouflaged instances. As can be seen from the figure, the state-of-the-art methods struggle to localize and segment camouflaged instances due to tiny size or extreme resemblance to the background. As also shown in Figure 14, the top three rows are immensely challenging examples, even for human. Meanwhile, the last two rows demonstrate the misclassification cases between camouflaged instances and non-camouflaged instances.

V. CONCLUSION AND OUTLOOK

In this paper, we study the interesting yet challenging problem, camouflaged instance segmentation. To this end, we collect a large-scale dataset, namely Camouflaged Object Plus Plus (CAMO++). We further provide an in-depth analysis on CAMO++ to demonstrate its diversity and complexity. We also conduct an extensive benchmark for the task of camouflaged instance segmentation. We evaluate state-of-the-art instance segmentation methods in various experimental settings. The results indicate that the existing methods well perform on the

TABLE IV: The results of training on CAMO++ and testing on CAMO-only images. The two best results are shown in **blue** and **red**, respectively.

Method	Backbone	Average Precision (AP)			AP Across Scales			Average Recall (AR)			AR Across Scales		
		AP	AP ₅₀	AP ₇₅	AP _S	AP _M	AP _L	AR ₁	AR ₁₀	AR ₁₀₀	AR _S	AR _M	AR _L
Mask RCNN [23]	ResNet50-FPN	24.6	53.3	20.8	5.3	17.3	27.0	26.2	35.0	35.1	6.7	25.2	38.3
Mask RCNN [23]	ResNet101-FPN	26.1	54.7	23.4	6.6	18.8	28.5	27.7	36.2	36.5	7.2	27.7	39.3
Mask RCNN [23]	ResNeXt101-FPN	31.3	63.3	27.7	10.5	20.9	34.5	3.5	40.0	40.2	11.1	28.5	43.8
Cascade RCNN [28]	ResNet50-FPN	25.9	53.4	22.4	4.3	18.4	28.4	27.6	37.1	37.3	4.4	27.9	40.4
Cascade RCNN [28]	ResNet101-FPN	26.9	54.5	24.2	6.5	19.5	29.3	28.3	38.6	38.8	11.1	28.0	42.1
Cascade RCNN [28]	ResNeXt101-FPN	33.8	64.8	33.0	9.0	25.9	36.6	33.7	46.5	47.2	15.6	38.5	50.0
MS RCNN [27]	ResNet50-FPN	26.9	53.2	25.6	9.1	19.6	29.0	27.1	33.2	33.3	12.8	25.5	35.7
MS RCNN [27]	ResNet101-FPN	28.6	54.6	27.7	10.0	22.3	30.6	28.3	35.1	35.2	13.9	28.5	37.4
MS RCNN [27]	ResNeXt101-FPN	32.9	62.4	32.0	15.0	26.1	35.1	31.9	40.2	40.4	16.1	33.2	42.7
RetinaMask [30]	ResNet50-FPN	23.5	50.9	19.2	10.7	19.1	25.1	26.4	35.5	35.8	12.2	29.7	37.8
RetinaMask [30]	ResNet101-FPN	25.4	54.0	21.9	16.2	18.7	27.4	28.3	37.1	37.4	23.9	31.6	39.1
RetinaMask [30]	ResNeXt101-FPN	28.1	58.3	24.4	17.9	22.1	29.9	31.4	39.7	40.0	20.0	34.3	41.9
YOLACT [34]	ResNet50-FPN	20.6	44.3	18.2	6.3	19.3	21.6	25.7	31.4	31.8	16.1	28.6	32.9
YOLACT [34]	ResNet101-FPN	23.1	46.9	20.7	13.7	18.4	24.9	28.3	33.8	33.8	20.0	26.8	35.9
CenterMask [36]	ResNet50-FPN	21.3	50.4	15.7	13.4	17.0	22.7	23.4	34.9	36.4	18.9	35.5	36.9
CenterMask [36]	ResNet101-FPN	24.6	54.6	20.2	14.6	17.9	26.7	26.4	36.1	36.4	20.0	32.6	37.6
CenterMask [36]	ResNeXt101-FPN	29.9	62.7	27.0	11.2	24.8	31.6	30.1	41.5	42.3	18.9	39.9	43.3
BlendMask [35]	ResNet50-FPN	25.9	55.5	21.6	13.4	20.6	27.6	28.2	36.9	37.0	17.8	30.1	39.2
BlendMask [35]	ResNet101-FPN	28.1	56.5	25.0	17.3	24.1	29.3	30.5	37.9	38.1	18.3	31.5	40.2
SOLO [41]	ResNet50-FPN	23.2	46.9	21.1	8.4	18.0	25.2	24.2	31.1	31.4	9.4	24.5	33.6
SOLO [41]	ResNet101-FPN	30.5	60.0	27.4	9.1	24.0	32.7	31.1	39.9	40.4	18.3	32.7	42.8
SOLO [41]	ResNeXt101-FPN	33.3	62.9	31.8	16.5	23.3	36.4	33.7	42.9	43.4	18.3	32.6	46.7
SOLO2 [42]	ResNet50-FPN	27.4	53.8	24.5	10.5	20.0	29.9	27.9	35.6	35.7	12.8	26.5	38.5
SOLO2 [42]	ResNet101-FPN	38.9	70.0	38.8	21.6	28.2	42.1	37.3	47.8	48.2	23.9	36.8	51.6
SOLO2 [42]	ResNeXt101-FPN	40.9	70.3	41.0	19.5	28.8	44.5	40.0	48.8	49.2	23.3	36.7	52.9
CondInst [43]	ResNet50-FPN	31.2	62.7	28.1	18.8	22.7	33.6	32.8	40.3	40.7	21.7	33.3	43.0
CondInst [43]	ResNet101-FPN	34.3	65.7	30.8	19.4	26.4	36.9	35.6	43.5	43.7	20.0	34.4	46.6

problem. In addition, the training non-camouflaged instances really help boost the performance of state-of-the-arts. However, there is still room for the improvement as we discussed in the failure cases. We believe that CAMO++ dataset can serve as a valuable benchmark for not only the camouflaged instance segmentation task, but also related tasks such as semantic camouflage segmentation, or video camouflaged instance segmentation.

In the future, we are exploring the impact of different factors on the given problem. For example, the contextual information may be helpful to detect and segment the camouflaged instance. In addition, we are looking at extending our work into the dynamic scenes, namely, videos. We would like to investigate the motion information in segmenting the camouflaged instance in the videos.

ACKNOWLEDGMENT

This work was funded by National Science Foundation (NSF) under Grant No. 2025234 and Vingroup Innovation Foundation, Vietnam (VINIF.2019.DA19). We also thank Thanh-An Nguyen, Minh-Quan Le, Hoang-Phuc Nguyen-Dinh, and Software Engineering Lab (University of Science, VNU-HCM) for their support in the annotation of the CAMO++ dataset. We gratefully acknowledge NVIDIA for the support of GPU.

REFERENCES

- [1] S. Singh, C. Dhawale, and S. Misra, "Survey of object detection methods in camouflaged image," *IERI Procedia*, vol. 4, pp. 351 – 357, 2013.
- [2] T.-N. Le, T. V. Nguyen, Z. Nie, M.-T. Tran, and A. Sugimoto, "Anabranch network for camouflaged object segmentation," *Journal of Computer Vision and Image Understanding*, vol. 184, pp. 45–56, 2019.
- [3] H. A. Qadir, Y. Shin, J. Solhusvik, J. Bergsland, L. Aabakken, and I. Balasingham, "Polyp detection and segmentation using mask r-cnn: Does a deeper feature extractor cnn always perform better?" in *International Symposium on Medical Information and Communication Technology*, 2019.
- [4] F. Ucar and D. Korkmaz, "Covidagnosis-net: Deep bayes-squeezenet based diagnosis of the coronavirus disease 2019 (covid-19) from x-ray images," in *Medical Hypotheses*, 2020.
- [5] H. H. Nguyen, F. Fang, J. Yamagishi, and I. Echizen, "Multi-task learning for detecting and segmenting manipulated facial images and videos," in *International Conference on Biometrics: Theory, Applications and Systems*, 2019.
- [6] H. H. Nguyen, J. Yamagishi, and I. Echizen, "Capsule-forensics: Using capsule networks to detect forged images and videos," in *International Conference on Acoustics, Speech and Signal Processing*, 2019.
- [7] M. Galun, E. Sharon, R. Basri, and A. Brandt, "Texture segmentation by multiscale aggregation of filter responses and shape elements," in *International Conference on Computer Vision*, Oct 2003, pp. 716–723.
- [8] L. Song and W. Geng, "A new camouflage texture evaluation method based on wssim and nature image features," in *International Conference on Multimedia Technology*, Oct 2010, pp. 1–4.
- [9] F. Xue, C. Yong, S. Xu, H. Dong, Y. Luo, and W. Jia, "Camouflage performance analysis and evaluation framework based on features fusion," *Multimedia Tools and Applications*, vol. 75, no. 7, pp. 4065–4082, Apr 2016.
- [10] Y. Pan, Y. Chen, Q. Fu, P. Zhang, and X. Xu, "Study on the camouflaged target detection method based on 3d convexity," *Modern Applied Science*, vol. 5, no. 4, p. 152, 2011.

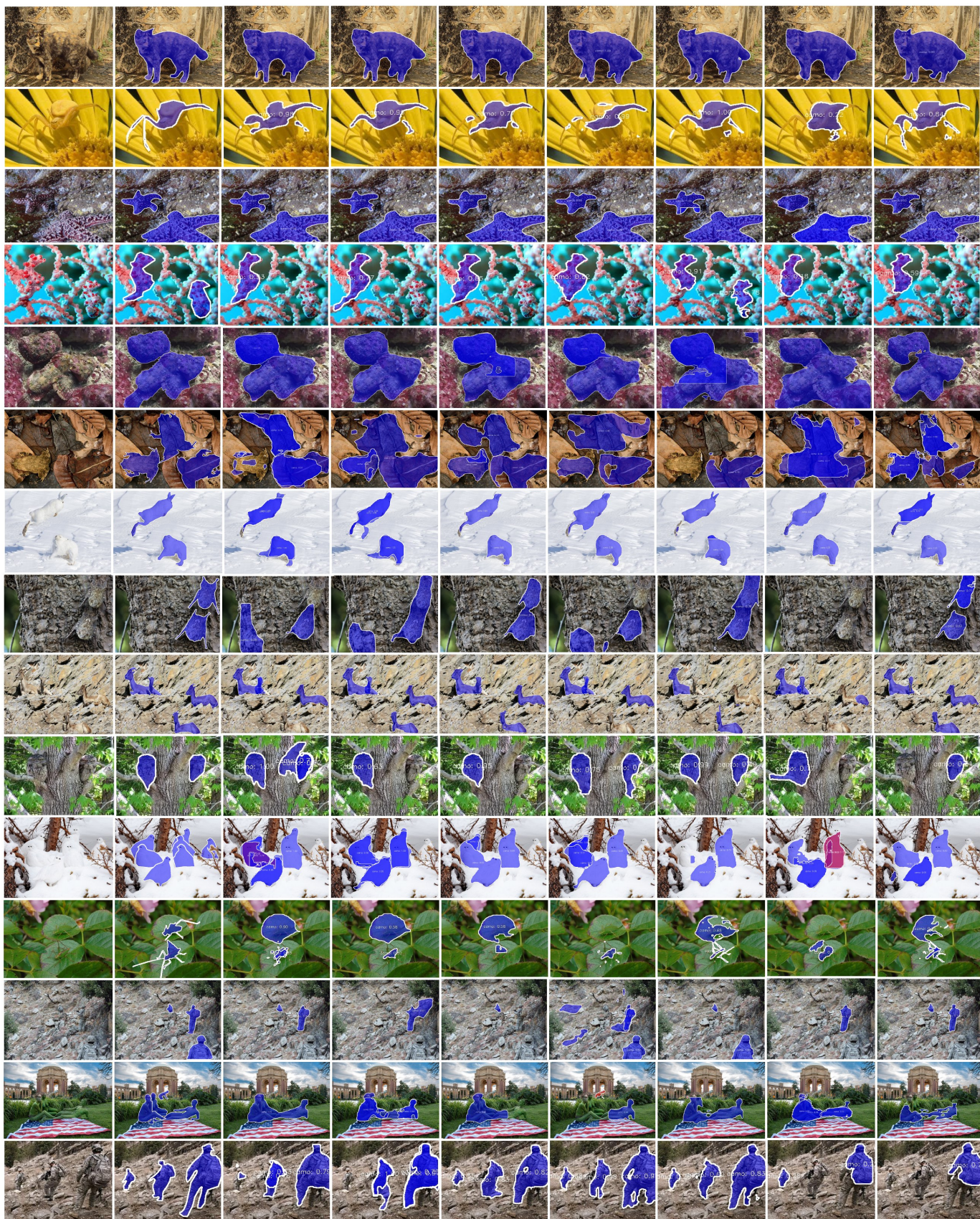


Fig. 13: Comparison of results from different methods. From left to right: the original image is followed by overlaid ground truth (blue: camouflage, red: non-camouflage) and the results of Mask RCNN [23], Cascade RCNN [28], MS RCNN [27], RetinaMask [30], YOLACT [34], CenterMask [36], and BlendMask [35]. Best viewed in color and with zoom.

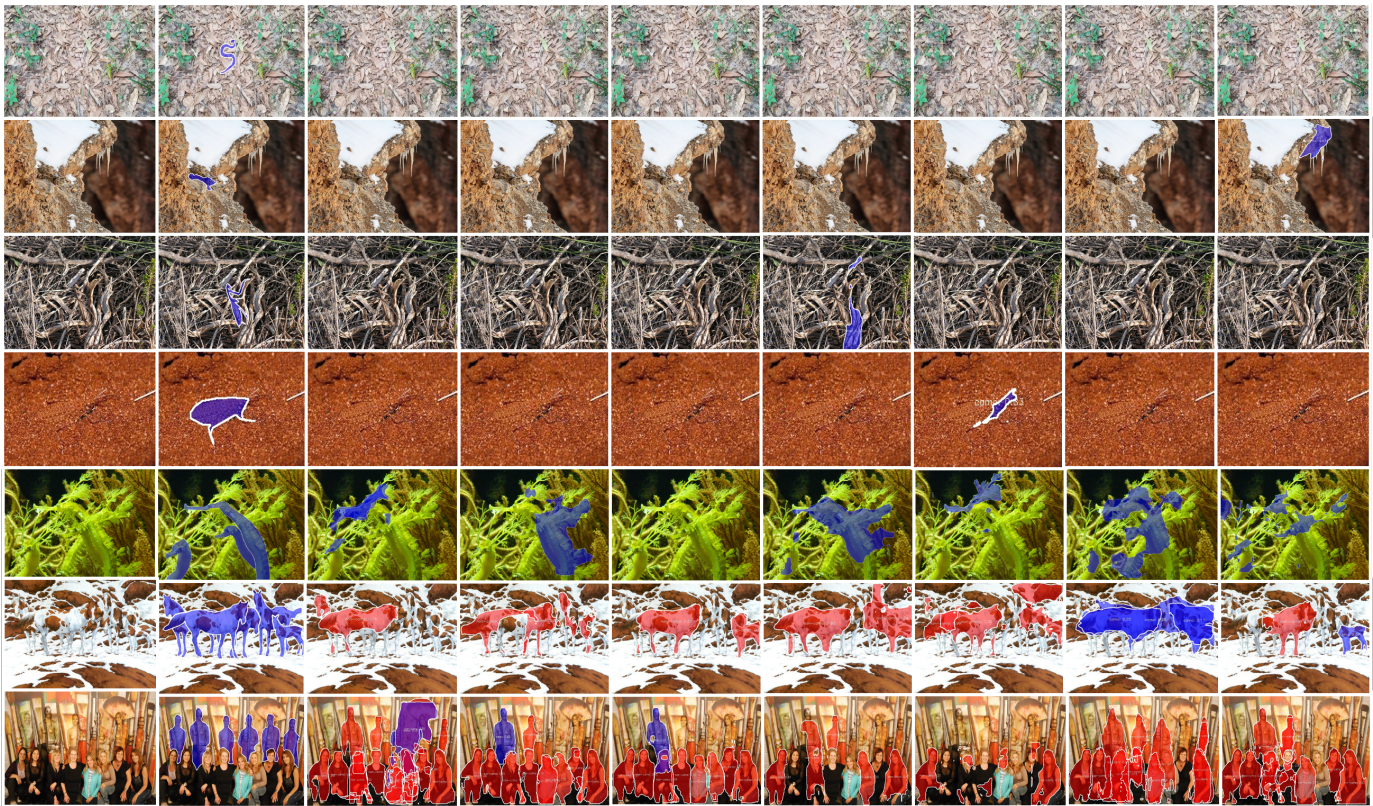


Fig. 14: Failure cases in camouflaged instance segmentation. From left to right: the original image is followed by overlaid ground truth (blue: camouflage, red: non-camouflage) and the results of Mask RCNN [23], Cascade RCNN [28], MS RCNN [27], RetinaMask [30], YOLACT [34], CenterMask [36], and BlendMask [35]. Best viewed in color and with zoom.

- [11] Z. Liu, K. Huang, and T. Tan, "Foreground object detection using top-down information based on em framework," *IEEE Transactions on Image Processing*, vol. 21, no. 9, pp. 4204–4217, Sept 2012.
- [12] A. W. P. Sengottuvelan and A. Shanmugam, "Performance of decamouflaging through exploratory image analysis," in *International Conference on Emerging Trends in Engineering and Technology*, July 2008, pp. 6–10.
- [13] J. Yin, Y. Han, W. Hou, and J. Li, "Detection of the mobile object with camouflage color under dynamic background based on optical flow," *Procedia Engineering*, vol. 15, no. Supplement C, pp. 2201 – 2205, 2011.
- [14] J. Gallego and P. Bertolino, "Foreground object segmentation for moving camera sequences based on foreground-background probabilistic models and prior probability maps," in *International Conference on Image Processing*, Oct 2014, pp. 3312–3316.
- [15] D.-P. Fan, G.-P. Ji, G. Sun, M.-M. Cheng, J. Shen, and L. Shao, "Camouflaged object detection," in *Conference on Computer Vision and Pattern Recognition*, 2020.
- [16] J. Yan, T.-N. Le, K.-D. Nguyen, M.-T. Tran, T.-T. Do, and T. V. Nguyen, "Mirronet: Bio-inspired camouflaged object segmentation," *arXiv preprint arXiv:2007.12881*, 2020.
- [17] A. Kirillov, E. Levinkov, B. Andres, B. Savchynskyy, and C. Rother, "Instanccut: from edges to instances with multicut," in *Conference on Computer Vision and Pattern Recognition*, vol. 3, 2017, p. 9.
- [18] E. Levinkov, J. Uhrig, S. Tang, M. Omran, E. Insafutdinov, A. Kirillov, C. Rother, T. Brox, B. Schiele, and B. Andres, "Joint graph decomposition & node labeling: Problem, algorithms, applications," in *Conference on Computer Vision and Pattern Recognition*, 2017.
- [19] X. Liang, L. Lin, Y. Wei, X. Shen, J. Yang, and S. Yan, "Proposal-free network for instance-level semantic object segmentation," *IEEE Transactions on Pattern Analysis and Machine Intelligence*, pp. 1–1, 2017.
- [20] Z. Zhang, S. Fidler, and R. Urtasun, "Instance-level segmentation for autonomous driving with deep densely connected mrfs," in *Conference on Computer Vision and Pattern Recognition*, 2016, pp. 669–677.
- [21] A. K. Konstantin Sofiiuk, Olga Barinova, "Adaptis: Adaptive instance selection network," in *International Conference on Computer Vision*, 2019.
- [22] J. Dai, K. He, and J. Sun, "Instance-aware semantic segmentation via multi-task network cascades," in *Conference on Computer Vision and Pattern Recognition*, 2016.
- [23] K. He, G. Gkioxari, P. Dollár, and R. Girshick, "Mask r-cnn," in *International Conference on Computer Vision*, 2017, pp. 2980–2988.
- [24] Y. Li, H. Qi, J. Dai, X. Ji, and Y. Wei, "Fully convolutional instance-aware semantic segmentation," in *Conference on Computer Vision and Pattern Recognition*, 2017.
- [25] S. Ren, K. He, R. Girshick, and J. Sun, "Faster r-cnn: Towards real-time object detection with region proposal networks," in *Advances in Neural Information Processing Systems*, 2015, pp. 91–99.
- [26] J. Dai, Y. Li, K. He, and J. Sun, "R-fcn: Object detection via region-based fully convolutional networks," in *Advances in Neural Information Processing Systems*, 2016, pp. 379–387.
- [27] Z. Huang, L. Huang, Y. Gong, C. Huang, and X. Wang, "Mask Scoring R-CNN," in *Conference on Computer Vision and Pattern Recognition*, 2019.
- [28] Z. Cai and N. Vasconcelos, "Cascade r-cnn: Delving into high quality object detection," in *Conference on Computer Vision and Pattern Recognition*, 2018.
- [29] S. Liu, L. Qi, H. Qin, J. Shi, and J. Jia, "Path aggregation network for instance segmentation," in *Conference on Computer Vision and Pattern Recognition*, 2018.
- [30] C.-Y. Fu, M. Shvets, and A. C. Berg, "RetinaMask: Learning to predict masks improves state-of-the-art single-shot detection for free," in *arXiv preprint arXiv:1901.03353*, 2019.
- [31] T.-Y. Lin, P. Goyal, R. Girshick, K. He, and P. Dollár, "Focal loss for dense object detection," in *International Conference on Computer Vision*, 2017, pp. 2980–2988.
- [32] X. Zhou, D. Wang, and P. Krähenbühl, "Objects as points," in *arXiv preprint arXiv:1904.07850*, 2019.
- [33] Z. Tian, C. Shen, H. Chen, and T. He, "Fcos: Fully convolutional one-

- stage object detection,” in *International Conference on Computer Vision*, October 2019.
- [34] D. Bolya, C. Zhou, F. Xiao, and Y. J. Lee, “Yolact: Real-time instance segmentation,” in *International Conference on Computer Vision*, 2019.
- [35] H. Chen, K. Sun, Z. Tian, C. Shen, Y. Huang, and Y. Yan, “Blendmask: Top-down meets bottom-up for instance segmentation,” in *Conference on Computer Vision and Pattern Recognition*, 2020.
- [36] Y. Lee and J. Park, “Centermask: Real-time anchor-free instance segmentation,” in *Conference on Computer Vision and Pattern Recognition*, 2020.
- [37] E. Xie, P. Sun, X. Song, W. Wang, X. Liu, D. Liang, C. Shen, and P. Luo, “Polarmask: Single shot instance segmentation with polar representation,” in *Conference on Computer Vision and Pattern Recognition*, 2020.
- [38] H. Ying, Z. Huang, S. Liu, T. Shao, and K. Zhou, “Embedmask: Embedding coupling for one-stage instance segmentation,” in *Conference on Computer Vision and Pattern Recognition*, 2020.
- [39] X. Chen, R. Girshick, K. He, and P. Dollár, “Tensormask: A foundation for dense object segmentation,” in *International Conference on Computer Vision*, 2019.
- [40] A. Gupta, P. Dollar, and R. Girshick, “Lvis: A dataset for large vocabulary instance segmentation,” in *Conference on Computer Vision and Pattern Recognition*, June 2019.
- [41] X. Wang, T. Kong, C. Shen, Y. Jiang, and L. Li, “SOLO: Segmenting objects by locations,” in *European Conference on Computer Vision*, 2020.
- [42] X. Wang, R. Zhang, T. Kong, L. Li, and C. Shen, “Solov2: Dynamic, faster and stronger,” in *Conference on Neural Information Processing Systems*, 2020.
- [43] Z. Tian, C. Shen, and H. Chen, “Conditional convolutions for instance segmentation,” in *European Conference on Computer Vision*, 2020.
- [44] K. He, X. Zhang, S. Ren, and J. Sun, “Deep residual learning for image recognition,” in *Conference on Computer Vision and Pattern Recognition*, June 2016, pp. 770–778.
- [45] S. Xie, R. Girshick, P. Dollár, Z. Tu, and K. He, “Aggregated residual transformations for deep neural networks,” in *Conference on Computer Vision and Pattern Recognition*, 2017, pp. 1492–1500.
- [46] T.-Y. Lin, M. Maire, S. Belongie, J. Hays, P. Perona, D. Ramanan, P. Dollár, and C. L. Zitnick, “Microsoft coco: Common objects in context,” in *European Conference on Computer Vision*, 2014, pp. 740–755.